A Novel Dual Energy CT-Based Attenuation Correction Method in PET/CT Systems: A Phantom Study

Original Article

Behnoosh Teimourian[1, 2], Mohammad Reza Ay[2,3,4], Mojtaba Shamsaei Zafarghandi[1], Hossein Ghadiri[2, 5]

[1]Faculty of Nuclear Engineering and Physics, Amir Kabir University of Technology, [2]Research Center for Science and Technology in Medicine, [3]Department of Medical Physics and Biomedical Engineering, [4]Research Institute for Nuclear Medicine, Tehran University of Medical Sciences, Tehran, Iran
[5]Department of Medical Physics, School of Medicine, Iran University of Medical Sciences, Tehran, Iran

(Received 17 October 2009, Revised 22 November 2009, Accepted 24 November 2009)

ABSTRACT

In present PET/CT scanners, PET attenuation correction is performed by relying on the information given by CT scan. In the CT-based attenuation correction methods, dual-energy technique (DECT) is the most accurate approach, which has been limited due to the increasing patient dose. In this feasibility study, we have introduced a new method that can implement dual-energy technique with only a single energy CT scan. The implementation was done by CT scans of RANDO phantom at tube voltages of 80 kV_P and 140 kV_P. The acquired data was used to obtain conversion curves (which scale CT numbers at different kV_P to each other), in three regions including lung tissue (HU<-100), soft tissue (-100<HU<200) and bone tissue (HU>200) for the combination of 80 kV_P /140 kV_P. Therefore, with having the CT image in one energy, we generate the CT image at the second energy (from now we call it virtual dual-energy technique) using these kV_P conversion curves. The attenuation map at 511 keV was generated using bilinear (the most commonly used method in commercially available PET/CT scanners), real dual-energy and virtual dual-energy technique in a polyethylene phantom. In the phantom study, the created attenuation map using mentioned methods are compared to the theoretical values calculated using XCOM cross section library. The results in the phantom data show 10.1 %, 4.2 % and 4.3 % errors for bilinear, dual-energy and virtual dual-energy techniques respectively. Further evaluation using a larger patient data is underway to evaluate the potential of the technique in a clinical setting.

Key Words: PET/CT, Dual Energy CT, Attenuation Correction

Iran J Nucl Med 2009;17(2):42-49

Corresponding author: Dr Mohammad Reza Ay, Department of Medical Physics and Biomedical Engineering, Tehran University of Medical Sciences, Tehran, Iran.
E-mail: mohammadreza_ay@tums.ac.ir

INTRODUCTION

Hybrid positron emission tomography/x-ray computed tomography (PET/CT) units have been designed and been commercially available since 2000 (1). The primary purpose of combining CT and PET scanners is for the precise anatomical localization of regions identified on the PET tracer uptake images. In addition, the use of CT images for CT-based attenuation correction (CTAC) reduces the overall scanning time and improves the precision of the attenuation correction factors (2).

Several physical factors can degrade the image quality and quantitative analysis of PET: the most important is photon attenuation in tissues, which can affect both the visual interpretation and quantitative analysis of PET data (3). With the introduction of hybrid PET/CT systems into the clinical setting, precise conversion from linear attenuation coefficients (LAC) of the tissues at effective CT energies (~ 60-80 keV, depending to the kV_p) to LAC at 511 keV , the energy of PET imaging, has become essential in order to apply accurate CTAC to the PET data. Several CTAC strategies have been developed, including scaling (4), segmentation (4), hybrid (segmentation and scaling) (4), bilinear (5), and dual-energy methods.

In the nominated methods, dual-energy technique (DECT) is most accurate one (6), but has been limited due to increasing patient dose resulting from two CT scans at two different kV_Ps. In this study we have introduced a new method that can implement dual-energy technique with only a single energy (kV_P) CT imaging. In this method, by having the CT image in one kV_P, we generate the CT image at the second kV_P. It should be emphasized that the aim of this method is to implement dual energy method for generating accurate attenuation map at 511 keV from CT images. The methodology is still under validation and need more assessment in clinical setting.

METHODS

CTAC methods

All CTAC methods in PET/CT systems require accurate conversion (energy mapping) from CT numbers to LACs at 511 keV. Several of conventional energy mapping methods are used which include scaling, segmentation, hybrid (scaling/segmentation), bilinear and dual-energy decomposition method.

In this study, we evaluated three methods to obtain 511 keV attenuation map (μmap): Bilinear which uses in the commercially available PET/CT scanner, DECT which is the most accurate method, and virtual DECT as the proposed low dose method.

Bilinear: In this method, as discussed by Bai et al (5), CT numbers in the range of $-1000 < HU \leq 0$ primarily represent regions that contain mixtures of air and water, whereas regions having CT numbers $HU > 0$ are those that contain mixtures of water and bone. The conversion from CT numbers at 140 kV_P to LACs at PET energy for each region is shown in table 1.

Table 1. The conversion from CT numbers at 140 kV_P to LACs at PET energy for two regions.

Region	Conversion from HU to LAC at PET energy (cm^{-1})
$-1000 < HU \leq 0$	$(1 + 1.00 \times 10^{-3} \times HU_x) \times 0.150$
$0 < HU$	$(1 + 7.04 \times 10^{-4} \times HU_x) \times 0.150$

DECT: In dual-energy method, attenuation correction is based on using two CT scans at different tube volatges but performed at the same time and patient position then uses these data to extract the individual photoelectric and Compton contributions in attenuation map as discussed by Guy et al (7).

It is well known that for photon energies less than 1.02 MeV, the overall linear

attenuation coefficient (μ^{tot}) is the sum of the photoelectric (μ^{pe}) and Compton (μ^{c}) components.

$$\mu^{tot} = \mu^{pe} + \mu^{c} \quad [1]$$

The photoelectric component is given by:

$$\mu^{pe} = K(\alpha m_e c^2)^{-3} \quad [2]$$

Where $\alpha = \frac{E}{m_e c^2}$, K is a constant, m_e is the electron mass and E is the photon energy.

The total Compton attenuation coefficient can be obtained using the Klein-Nishina formula, as shown in Equation [3]:

$$\mu^{c} = X\left[\frac{2(1+\alpha)^2}{\alpha^2(1+2\alpha)} + \frac{\ln(1+2\alpha)}{\alpha}\left(\frac{1}{2} - \frac{1+\alpha}{\alpha^2}\right) - \frac{1+3\alpha}{(1+2\alpha)^2}\right] \quad [3]$$

Where $X = \frac{3n_e\sigma^0}{4}$ and σ^0 is the classical cross section. So, if the two incident photon beams have the energies of E_1, and E_2,, with corresponding attenuation values of μ_1 and μ_2, the total linear attenuation coefficient (μ_3) at the scaling energy, E_3 is given by:

$$\mu_3 = \frac{(\mu_1 E_2^{-3} - \mu_2 E_1^{-3})}{(Y_1 E_2^{-3} - Y_2 E_1^{-3})} Y_3 + \frac{(\mu_1 Y_2 - \mu_2 Y_1)}{(Y_2 E_1^{-3} - Y_1 E_2^{-3})} E_3 \quad [4]$$

Where $\alpha_n = \frac{E_n}{m_e c^2}$, and:

$$Y_n = \left[\frac{2(1+\alpha_n)^2}{\alpha_n^2(1+2\alpha_n)} + \frac{\ln(1+2\alpha_n)}{\alpha_n}\left(\frac{1}{2} - \frac{1+\alpha_n}{\alpha_n^2}\right) - \frac{1+3\alpha_n}{(1+2\alpha_n)^2}\right]$$

Virtual DECT: In this proposed method, with having the CT image in one tube volate and generating the CT image at the second tube voltage, DECT technique is implemented using the real and virtual image, as described above.

Phantom Studies

RANDO Phantom

The RANDO phantom (RANDO Alderson; Phantom Laboratory, Salem, NY, (8)) is an invaluable aid in radiotherapy treatment planning. There are two RANDO models: The RANDO woman and the RANDO man. The woman represents a 163cm tall and 54kg and the man represents a 175cm tall and 73.5kg (figure 1). Neither have arms or legs. Breast accessories are available for both models.

Figure 1. Photograph of RANDO phantom.

Like the sectional phantoms, the RANDO phantoms are constructed with a natural human skeleton cast inside material that is radiologically equivalent to soft tissue. The RANDO lungs are molded to fit the contours of the natural human rib cage. The lower-density material in the RANDO lungs is designed to simulate human lungs in a median respiratory state.

For this study, the RANDO phantom was scanned by a LightSpeed VCT scanner (GE Healthcare Milwaukee, USA) at 80 and 140 kV_P tube voltages and with tube current of 300 mA. Figure 2 shows the whole body coronal CT images of RANDO phantom at the 80 and 140 kV_P tube voltages.

Figure 2. The whole body coronal CT images of RANDO phantom at 80 kV_P (right) and 140 kV_P (left).

The analysis on the acquired images was done by AMIDE (9) image viewer. More than 200 different ROIs were selected in each image and the mean CT numbers for each ROI at one kV_P was plotted versus the same values at another kV_P. Finally the best curve was fitted for each plot to obtain kV_P Conversion Curves (which scale CT numbers at different tube voltages to each other), in three regions including lung tissue ($HU \leq -100$), soft tissue ($-100 < HU < 200$) and bone tissue ($HU \geq 200$). This classification improves the precision of the resulted kV_P conversion curves.

The kV_P Conversion curves have been obtained for the combination of 80 kV_P /140 kV_P . It should be noted that in dual energy method, the accuracy of estimating attenuation map at 511 keV is directly related to the difference of the pair energies used in each combination (8). The calculated kV_P Conversion Curves can be used for generation of virtual CT image in other kV_Ps. Having the CT image of a patient in one energy and generating the second image in another energy, we are now able to implement the dual energy technique which is called the virtual dual-energy method.

Polyethylene Phantom

A polyethylene cylindrical phantom (250±0.5 mm diameter) was constructed. This phantom consisted of 16 cylindrical holes (20±0.5 mm diameter) with four holes in the middle (5±0.5 mm diameter) filled with air. One of the 16 holes was filled with water and the rest with various concentrations of K_2HPO_4 solution varying from 60 mg/cc to 1800 mg/cc (LAC ranging from 0.1 to 0.2 cm^{-1} at 511 keV) to simulate different biological tissues (figure 3).

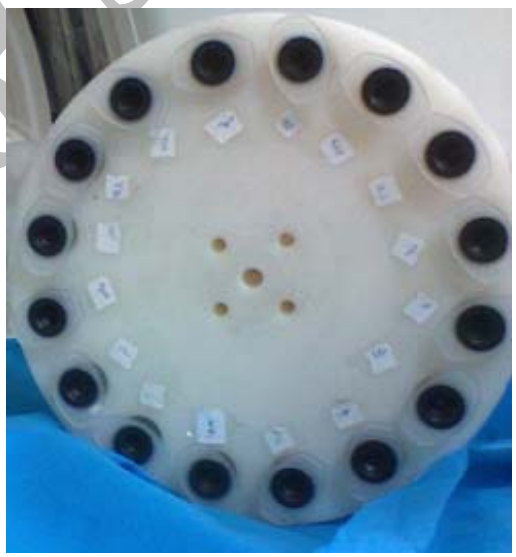

Figure 3. Photograph of Polyethylene phantom.

This phantom was scanned on the LightSpeed VCT scanner at two different tube voltages of 80 and 140 kV_P and tube current of 400 mA with 1 sec rotation speed. The acquired data was used to generate μmaps using the three mentioned CTAC methods: The acquired CT image at 140 kV_P was converted to μmaps using the bilinear method and the CT images at 80 and 140

kV_P were used to implement DECT technique.

In the proposed method, by using the kV_P Conversion Curves, which have been obtained from the CT images of RANDO phantom, phantom image at 80 kV_P was derived from 140 kV_P. Then attenuation map at PET energy was generated using the CT images at 80 kV_P (which was derived from 140 kV_P) and 140 kV_P . This is the virtual DECT method. As the noise of the CT image is lower in higher kV_Ps, CT image at 80 kV_P was derived from 140 kV_Ps.

The theoretical LAC at 511 keV for each concentration of the K_2HPO_4 solution was computed using the XCOM photon cross section library (10), and considered as gold standard.

Generation of μmap and Assessment Strategy

The reconstructed CT images (512×512 matrix size) were at first down-sampled to 128×128 and then smoothed using a 5-mm Gaussian kernel to match the resolution of the PET images. Then bilinear, dual-energy and virtual dual-energy methods were used to convert CT image to an attenuation map (μmap) at 511 keV.

A ROI-based quantitative analysis was performed on phantom data for the assessment of the accuracy of different energy mapping strategies. Several ROIs were defined on regions of the μmap corresponding to different concentrations of the K2HPO4 solutions and the mean LAC was computed. The result was then compared to the theoretical LAC estimated using the XCOM photon cross section library (10).

RESULTS AND DISCUSSION

RANDO Phantom

The kV_P conversion curves, which obtained from CT scans of RANDO phantom at tube voltages 80 and 140 kV_P, for different tissue types including lung tissue, soft tissue, and bone tissue are shown in figure 4. Table 2 presents the conversion equations, that convert the CT images at 140 kV_P to CT images at 80 kV_P , for mentioned tissue types. These conversion equations are used to generate the CT images at 80 kV_P from the acquired CT images at 140 kV_P using the MATLAB.

Table 2. The conversion equations that convert the CT images at 140 kV_P to CT images at 80 kV_P for different tissue types.

Tissue Type	Conversion Equation from 140 kV_P to 80 kV_P
Lung Tissue (HU ≤ -100)	$HU_{80kVp} = (1.083 \times HU_{140kVp}) + 94.60$
Soft Tissue (-100 < HU < 200)	$HU_{80kVp} = (1.529 \times HU_{140kVp}) + 9.911$
Bone Tissue (HU ≥ 200)	$HU_{80kVp} = (1.431 \times HU_{140kVp}) + 33.45$

Polyethylene Phantom

Figure 5 shows two CT images at 80 kV_P. One is the original CT image and the other one is the generated CT image from 140 kV_P using the kV_P conversion equations.

The original CT image at 140 kV_P and μmaps of the phantom generated using different energy mapping techniques including bilinear, DECT, and virtual DECT are shown in figure 6. Table 3 summarizes calculated LACs at 511 keV for the different regions of phantom and the reference values extracted from the XCOM cross section library. The percentage relative differences between the calculated LAC using different energy mapping methods and theoretical values for different concentrations of K_2HPO_4 are also presented in table 3. The average percentage relative difference in all regions calculated using bilinear, dual-energy and virtual dual-energy methods are 10.1%, 4.2%, 4.3% respectively. Therefore, the accuracy of virtual DECT is almost equal to DECT method.

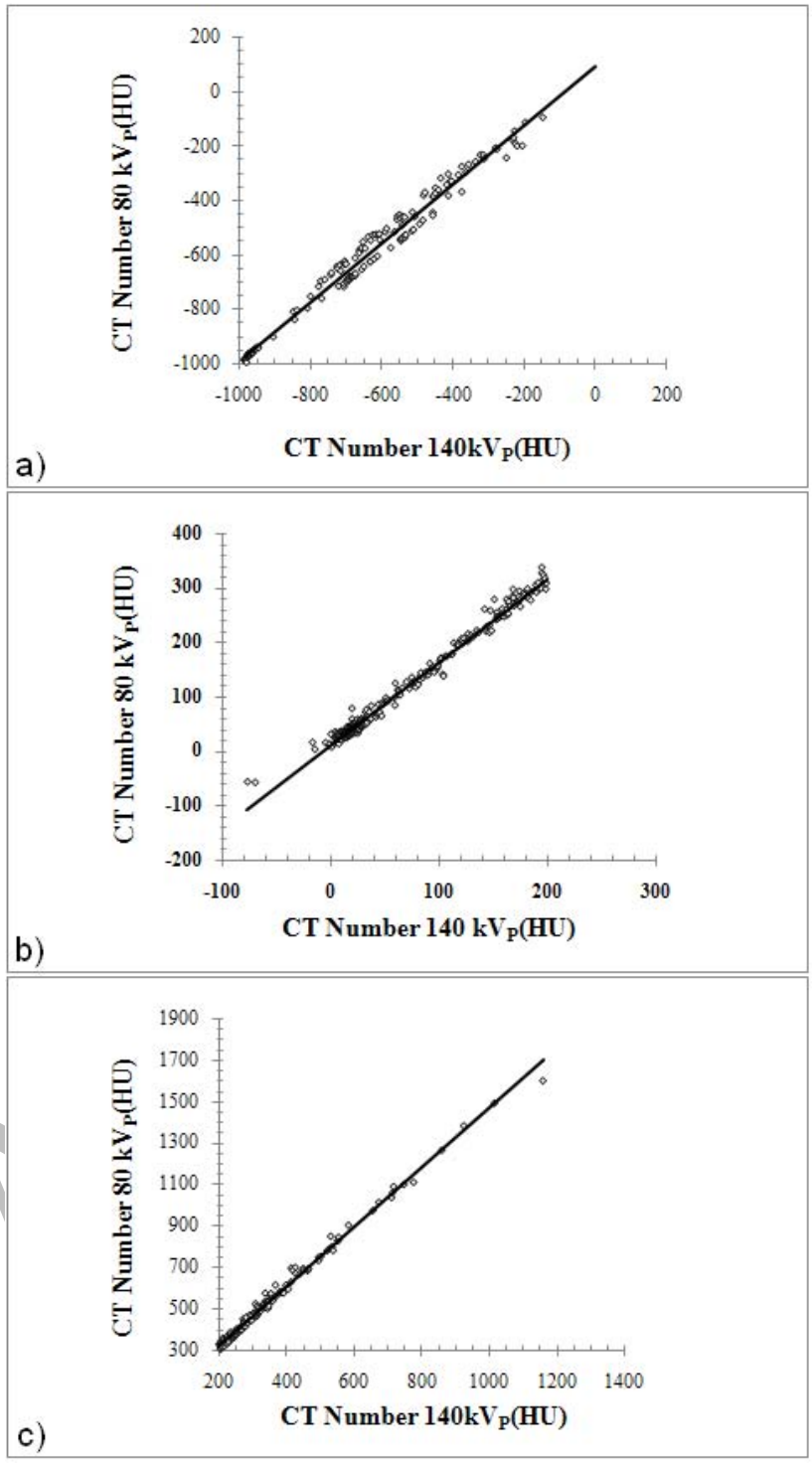

Figure 4. The dots (symbol ◇) show the mean CT numbers of each ROI at 80 kV_P versus the corresponding values at 140 kV_P. The solid line is the fitted curve to the dot plots in different tissue types including a) soft tissue, b) lung tissue, and c) bone tissue.

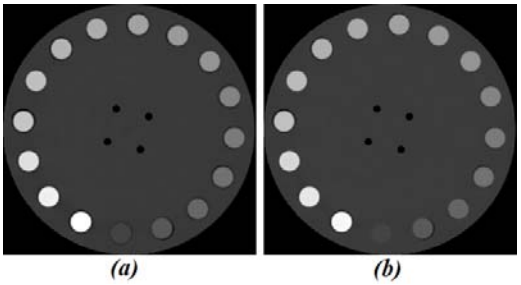

Figure 5. The CT images at 80 kV_P , a) Original CT image, b) Generated CT image from CT 140 kV_P (virtual image).

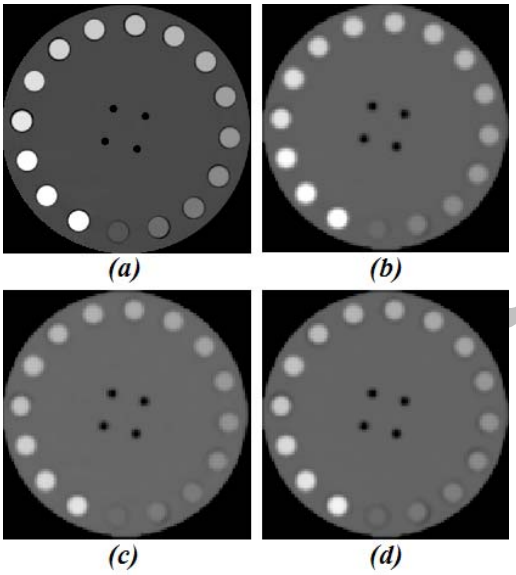

Figure 6. (a) Original CT image at 140 kV_P (b) generated attenuation maps at 511 keV using bilinear (c), dual energy (80 and 140 kV_Ps) (d) and virtual dual-energy.

Figure 7 shows difference images obtained by subtracting generated μmap images using the bilinear and virtual DECT techniques and the reference image. The obtained μmap image using DECT method has been considered as reference image.

Table 3. Comparison of calculated LACs at 511 keV using different CTAC method and the theoretical values computed using the XCOM photon cross section library for different regions within the phantom.

C [†](mgr/cc)	LAC at 511 keV (PRD[*])			
	XCOM	Bilinear	DECT	Virtual DECT
Water	0.096	0.096 (0.0)	0.097 (1.0)	0.097 (1.0)
120	0.102	0.107 (4.9)	0.105 (2.9)	0.104 (2.0)
180	0.106	0.113 (6.6)	0.105 (0.9)	0.108 (1.9)
240	0.109	0.121 (11.0)	0.113 (3.7)	0.115 (5.5)
300	0.112	0.126 (12.5)	0.117 (4.5)	0.117 (4.5)
360	0.116	0.131 (12.9)	0.121 (4.3)	0.121 (4.3)
480	0.123	0.140 (13.8)	0.128 (4.1)	0.129 (4.9)
540	0.126	0.144 (14.3)	0.130 (3.2)	0.131 (4.0)
600	0.129	0.148 (14.2)	0.133 (3.1)	0.134 (3.9)
660	0.133	0.153 (15.0)	0.136 (2.3)	0.139 (4.5)
720	0.136	0.157 (15.4)	0.139 (2.2)	0.141 (3.7)
840	0.143	0.163 (14.0)	0.143 (0.0)	0.147 (2.8)
900	0.147	0.166 (12.9)	0.145 (1.4)	0.148 (0.7)
1200	0.164	0.180 (12.9)	0.154 (6.1)	0.158 (3.7)
1500	0.181	0.188 (3.9)	0.159 (12.1)	0.165 (8.8)
1800	0.199	0.198 (0.5)	0.168 (15.6)	0.174 (12.6)

[†]Concentration of K2HPO4 in solution
[*]Percentage Relative Difference (%)

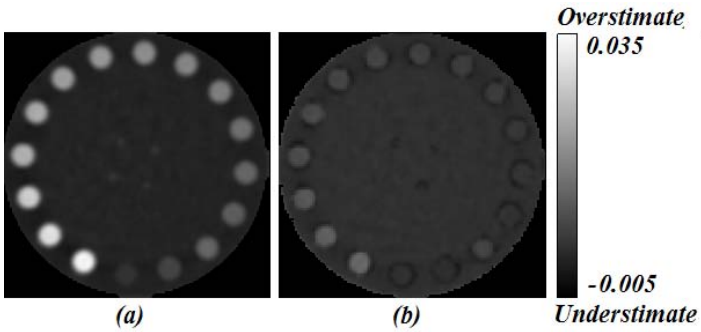

Figure 7. Difference image between obtained μmaps (a) DECT and bilinear (b) DECT and virtual DECT.

CONCLUSION

Among different CTAC methods of PET data, the bilinear method is the common used method in most commercial PET/CT scanners. This method has an acceptable accuracy in lung and soft tissue, but overestimates in bone tissue. Also, the dual-energy method has a good estimation of attenuation coefficients at 511 keV for all tissues, but the use is limited because of its high dose. In this feasibility study we have introduced a new method that can implement dual-energy technique with only a single energy (kV_P) CT imaging.

As shown in table 3, that dual-energy and virtual dual-energy have the low errors in obtaining LACs at 511 keV (4.2 % and 4.3 % respectively).

In this feasibility study, we presented the results showing the virtual dual-energy approach has not only the same performance as dual energy technique but has additional potential advantages of a lower patient dose. Further evaluation using a clinical PET/CT database is underway to evaluate the potential of the technique in a clinical setting.

ACKNOWLEDGEMENTS

This work has been supported by the Research Center for Science and Technology in Medicine, Tehran University of Medical Sciences.

REFERENCES

1. Townsend DW, Beyer T, Blodgett TM. PET/CT scanners: a hardware approach to image fusion. Semin Nucl Med. 2003;33(3):193-204.
2. Beyer T, Townsend DW, Brun T, Kinahan PE, Charron M, Roddy R et al. A combined PET/CT scanner for clinical oncology. J Nucl Med. 2000;41(8):1369-1379.
3. Zaidi H, Hasegawa B. Determination of the attenuation map in emission tomography. J Nucl Med. 2003;44(2):291-315.
4. Kinahan PE, Townsend DW, Beyer T, Sashin D. Attenuation correction for a combined 3D PET/CT scanner. Med Phys. 1998;25(10):2046-2053.
5. Bai C, Shao L, Da Silva AJ, Zhao Z. A generalized model for the conversion from CT numbers to linear attenuation coefficients. IEEE Trans Nucl Sci. 2003;50(5):1510-1515.
6. Shirmohammad M, Ay MR, Sarkar S, Rahmim A, Zaidi H. Comparative assessment of different energy mapping methods for generation of 511-keV attenuation map from CT images in PET/CT systems: A phantom study. Proceedings of the 4th European Conference of the International Federation for Medical and Biological Engineering, 2008 Nov 23-27; Antwerp, Belgium.
7. Guy MJ, Castellano-Smith IA, Flower MA, Flux GD, Ott RJ, Visvikis D. DETECT-Dual energy transmission estimation CT-for improved attenuation correction in SPECT and PET. IEEE Trans Nucl Sci. 1998;45:1261-1267.
8. RANDO phantom website. URL: http://www.rsdphantoms.com
9. AMIDE image viewer software. URL: http://amide.sourceforge.net
10. Berger MJ, Hubbell JH, Seltzer SM, Chang J, Coursey JS, Sukumar R et al. XCOM:photon cross sections database. NBSIR 87-3597. URL: http://physics.nist.gov/PhysRefData/Xcom/Text/XCOM.html